Palaeogeography, Palaeoclimatology, Palaeoecology 432 (2015) 15–28

Contents lists available at ScienceDirect

Palaeogeography, Palaeoclimatology, Palaeoecology

journal homepage: www.elsevier.com/locate/palaeo

Redox conditions in the end-Early Triassic Panthalassa

Satoshi Takahashi [a,*], Shin-ichi Yamasaki [b], Kazuhiro Ogawa [c], Kunio Kaiho [c], Noriyoshi Tsuchiya [b]

[a] Department of Earth and Planetary Science, University of Tokyo, Hongo 7-3-1, Tokyo, Japan
[b] Graduate School of Environmental Studies, Tohoku University, Aramaki-Aza-Aoba 6-6-20, Sendai, Japan
[c] Graduate School of Science, Tohoku University, Aramaki-Aza-Aoba 6-3, Sendai, Japan

ARTICLE INFO

Article history:
Received 22 January 2015
Received in revised form 16 April 2015
Accepted 21 April 2015
Available online 12 May 2015

Keywords:
Early Triassic
Trace element
Pyrite framboid
Sulphur isotope
Redox conditions
Deep-sea

ABSTRACT

This study focuses on an upper Lower Triassic (Spathian) to lowermost Middle Triassic (Anisian) section representing the central Panthalassic deep sea. Analysed organic carbon isotope ratio ($\delta^{13}C_{org}$) records from the section demonstrate that lower values in the Spathian increase by up to 6‰ at the Spathian–Anisian transition. This trend accords with the carbonate carbon isotope ($\delta^{13}C_{carb}$) record from shallow-water carbonate sections. Most horizons during late Spathian–early Anisian show features of redox conditions of not fully oxic but dysoxic conditions, inferred from low Mn, U, V, Mo and euhedral pyrite-dominated occurrences. Conversely, in the end-Spathian black-coloured beds and underlying siliceous claystone beds, relatively higher concentrations of redox-sensitive elements such as U, V, Mo and abundant pyrite framboids are detected. As enrichment factors of redox-sensitive elements are not much higher than the typical anoxic–sulphidic trend and large pyrite framboids are found, these trends suggest suboxic rather than strong anoxic conditions. These oxygen-poor conditions coincide with carbon isotope minimum values at the late Spathian. At the same time, reducing seawater conditions have been also reported in from continental sections. These coincidences imply global environmental perturbations that may have been related to the delayed recovery of life after the end-Permian mass extinction.

1. Introduction

After the Permian–Triassic mass extinction, marine ecosystems experienced several stressful environments through the Early Triassic, finally recovering during the Anisian in the early Middle Triassic (e.g., Chen and Benton, 2012; Algeo et al., 2013). The process that delayed recovery of marine animals in the Early Triassic is an important question that needs to be answered. The Early Triassic was characterised by carbon isotope perturbations (Fig. 1; Payne et al., 2004; Galfetti et al., 2007; Sun et al., 2012). The features of carbon isotopes combined with biostratigraphy provide a useful tool for global chronological correlation. Around the Early Triassic to Middle Triassic transition (Olenekian [Spathian] to Anisian), a significant swing from late Spathian minimum values to an early Anisian positive spike is observed in the carbonate carbon isotope ratio ($\delta^{13}C_{carb}$) in shallow-water carbonate sections (Fig. 1). These carbon isotope features were labelled by Song et al. (2013, 2014), who defined N1–N4 after first initial negative and P1–P4 after first initial positive values (Fig. 1). The minimum values at late Spathian and following early Anisian maximum values are named N4 and P4, respectively.

The recovery pattern after the mass extinction differs on the basis of the clades of conodonts, ammonites and possibly other nekton animals that diversified more rapidly than others in the Smithian. However, at a time similar to that of the late Spathian $\delta^{13}C_{carb}$ minimum values and the following increasing trend, the diversity of ammonites and conodonts decreased (Orchard, 2007; Stanley, 2009). Then, marine animals began to diversify after the early Anisian (e.g., as compiled by Chen and Benton [2012] and Sun et al. [2012]). Warm temperature conditions were implied by $\delta^{18}O$ of conodont apatite, but this trend was not more significant than the increases in $\delta^{18}O$ at the Griesbachian–Dienerian and Smithian–Spathian transitions (Romano et al., 2012; Sun et al., 2012). Stressful oceanic conditions during the Spathian have been reported in several regions. Oxygen-poor seawater conditions are one possible candidate for the cause of these temporal decreases and the delay of recovery because geochemical anoxic evidence, such as organic molecules and redox-sensitive elements, has been reported from some late Spathian sedimentary horizons from the Panthalassic ocean, Boreal deep sea and continental shelf carbonates (Takahashi et al., 2009a; Marenco et al., 2012; Grasby et al., 2012; Wignall et al., 2010; Song et al., 2012; Saito et al., 2014; Tian et al., 2014).

Among these sedimentary settings, the Panthalassic deep ocean provides widely extended environmental information (Fig. 1). This study focuses on such pelagic deep-sea sediments from Japanese accretionary complexes (Matsuda and Isozaki, 1991; Ando et al., 2001; Fig. 1) and presents continuous stable carbon isotope ratio of organic matter ($\delta^{13}C_{org}$) curves across a Spathian–Anisian boundary section, namely the Momotaro–Jinja section (Mj section) in central Japan. This section preserves a lithological change from Spathian siliceous claystone to Anisian chert (Yamakita, 1987; Kakuwa, 1996; Isozaki, 1997). The

* Corresponding author. Tel.:+81 3 5841 4538.
E-mail address: stakahashi@eps.s.u-tokyo.ac.jp (S. Takahashi).

http://dx.doi.org/10.1016/j.palaeo.2015.04.018
0031-0182/

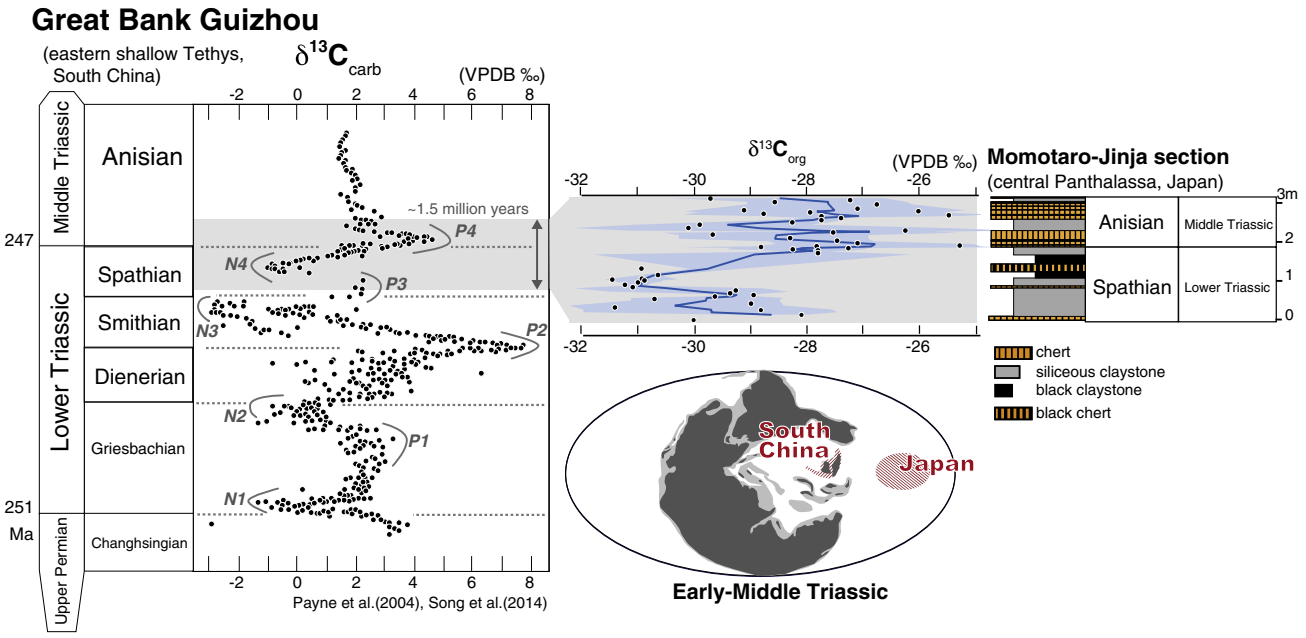

Fig. 1. Carbon isotopic profiles during the Early Triassic and Middle Triassic from a shallow-water carbonate section (Great Bank of Guizhou, South China; Payne et al., 2004) and a deep-water siliceous sedimentary section (Momotaro–Jinja section, central Japan; this study). A palaeogeographic map (by Ziegler et al., 1998) showing depositional areas of Lower–Middle Triassic sediment from South China and Japan is also shown. For $\delta^{13}C_{org}$ of the Momotaro–Jinja section, a three-point running mean (blue line) and ±2 standard error (sky blue area) are shown.

deposition of these claystones is thought to reflect a decrease in biotic silica deposition and widespread oxygen-poor conditions during the Late Permian and Early Triassic (Isozaki, 1997; Algeo et al., 2010; Takahashi et al., 2009b; Algeo et al., 2011), and the recommencement of chert deposition is thought to reflect the process of biotic recovery, mainly silicic radiolarian productivity. Furthermore, Takahashi et al. (2009a) reported late Spathian development of somewhat-reducing water based on geochemical evidence, such as high dibenzothiophene (sulphur-bonded organic compounds) concentrations and high S/C ratios, and postulated that the development of oxygen-poor ocean was one possible reason for the delayed recovery in pelagic Panthalassa. Herein, we also present trace element compositions, sulphide mineral occurrences and their isotope ratios ($\delta^{34}S_{sulphide}$) for further discrimination of late Spathian redox conditions.

2. Geological setting and lithology

The Mj section (first named by Yao and Kuwahara (1997) after the Momotaro–Jinja shrine), is located in the Mino Belt of central Japan and consists of Jurassic accretionary complexes (Fig. 2). The 7.5-m-thick Mj section is composed of the following lithological facies in ascending order: 1.5-m-thick grey siliceous claystone, 1.5-m-thick red siliceous claystone (cut by a small fault at 0.25 m), 1.25-m-thick grey siliceous claystone interbedded with two chert beds, 0.16- and 0.24-m-thick black chert beds and 1.5-m-thick alternating grey chert and siliceous claystone. The age of the section has been examined using radiolarian and conodont biostratigraphy (Yao and Kuwahara, 1997; Takahashi et al., 2009a), which indicates that the section ranges from Spathian (upper Olenekian) to lower Anisian. The Lower Triassic–Middle Triassic transition (equals Spathian–Anisian) is at the contact between the black chert and overlying grey chert, as indicated by the *Parentactinia nakatsugawaensis*/*Hozmadia gifuensis* zone boundary (the first occurrence of *Triassocampe* sp., which characterises the *H. gifuensis* assemblage; Figs. 2 and 3).

This study focuses on the 3.3-m Spathian–Anisian transition interval, from 2 m below to ca. 1.3 m above the Olenekian–Anisian boundary (OAB) (Figs. 2 and 3). This interval is composed of dark greenish-grey-coloured siliceous claystone beds (1.1 m thick, Beds 1–17), a thick black chert bed (Bed 19) interbedded with black claystone, overlying dark greenish-grey-coloured siliceous claystone beds (Beds 21–24), muddy chert and chert beds (Beds 26–34), siliceous claystone beds (Beds 34–39) and muddy chert and chert beds (Beds 40–52). The upper limit of the section is the small fault. The base of this interval corresponds to the first occurrence of a chert bed interbedded in grey siliceous claystone beds (Bed group 7 of Takahashi et al., 2009a) overlying the red siliceous claystone bed of the lower part of the Mj section (Bed group 5 of Takahashi et al., 2009a). The base of the Anisian strata is placed between the black chert of Bed 19 and the muddy chert of Bed 26 (Yao and Kuwahara, 1997).

3. Methods

Samples were collected from the study interval in the Mj section. Weathered samples and samples with modern vegetation were avoided. Samples were sliced and polished on cut surfaces for observation. Cut surfaces were photographed using a flat-head scanner (Epson GTX970) with colour separation guides (Kodak Q-13). For sampling reproduction, rock colour information (Lab colour space) was measured by Adobe Photoshop software (Table 1). Significant white- and black-coloured carbonaceous veins were observed in Beds 4, 20 and 53 (a typical example of Bed 20 is shown in Fig. 4). These samples are enriched in Si, Mn, Fe and Ca, which was confirmed by inductively coupled plasma mass spectrometry (ICP-MS) analysis (see underlined lists in Table 1) and X-ray microscope observations using a Horiba XGT2700. Because of these contaminations to the sedimentary chemical compositions, we did not include these samples in the following vertical plots.

3.1. Organic carbon isotope ratios

The samples from the Mj section were powdered and then treated repeatedly with 6 N HCl to remove all carbonates and other acid-soluble minerals. Typically, 10–30 mg of sample powder was sealed in foil for the isotope analyses. Then, the carbon isotope ratios of the